Inelastic neutron scattering of Na-zeolite A with *in situ* ammoniation: an examination of initial coordination

A. G. Seel,*[a] A. Sartbaeva,[a] A. J. Rammirez-Cuesta[b] and P. P. Edwards[a]

Received 24th February 2010, Accepted 26th April 2010
DOI: 10.1039/c003567j

The detection and rationalization of the coordination of low concentrations of ammonia within Na-zeolite A is carried out by the application of inelastic neutron scattering (INS), using inverse geometry time of flight spectrometry to study the partial phonon density of states of *in situ* ammoniated Na-zeolite A. The experimental spectra are subsequently characterised by density functional calculations, incorporating pre-optimisation by geometric simulation. We find that at a concentration of four ammonia molecules per α-cage, the ammonia molecule coordinates with extra-framework Na^+ cations and gives rise to three structured regions in the INS spectrum. We show that these regions correspond to translational, librational and tilting motions of the ammonia molecule. These results are in agreement structurally with previous studies of ammonia within a zeolite, and thus show that INS is a valid technique for such investigations.

1. Introduction

We present in this work the first study tailored to the detection of coordinated ammonia incarcerated within a zeolite (Na-zeolite A) by inelastic neutron scattering (INS). Zeolites are a family of crystalline aluminosilicate minerals consisting of conjoined tetrahedra of TO_4 where T = Si, Al. The microporosity and low densities of zeolite frameworks have made them some of the most interesting and highly utilised materials for the encapsulation, adsorption and storage of small molecules.[1,2] In addition to the physical study of confinement,[3,4] applications of zeolites in the petrochemical[5] and energy industries have increased greatly in the last half-century, with the fabled 'hydrogen economy' rising to the forefront of physicochemical objectives.[6–8] In view of this, many studies on the storage and interaction of small, hydrogen-containing molecules (such as H_2,[9,10] CH_4[11] and NH_3[12]) in micropores have been undertaken. The latter has been driven by the suitability of ammonia as a fuel source[13] and hydrogen store.[14] Relatively little study, however, has been conducted on zeolites containing *low* concentrations of these molecules. This is an important area of research for examining initial coordination sites of small molecules, giving an insight into possible modes of transport through the zeolite system.

One of the inherent problems with studies of small molecules within zeolites, particularly at low concentrations, is the spectroscopic isolation of such species from the zeolite framework. The distribution of a small number of guest molecules within a large cavity, as in zeolites, also raises the issue of disorder (where the number of possible coordination sites exceeds that of the coordinating species), and thus techniques that examine the local environment of the guest molecule rather than the structural average must be employed. Previous studies that satisfy these criteria mainly center around magnetic resonance techniques.[15,16] Elucidation of local structure by NMR may become difficult in the presence of strongly paramagnetic centres, such as may exist in d- and f-block exchanged zeolites, and thus the application of techniques that are independent of electron/spin density to such systems would be beneficial. INS has previously been used to examine the vibrational modes of organic molecules within zeolite cages,[17–19] and we note that INS spectra are easily manipulated making the removal of a background (in our case that of the sample container and the zeolite pre-ammoniation) trivial. This enables the collection of fingerprint spectra relating only to the guest molecule. INS is shown to be able to characterize low wavelength (neutron energy loss) regions of the vibrational spectrum; a region previously not investigated by IR spectroscopy.[20] Raman techniques may also be used to study the vibrational structure of absorbed molecules in zeolites,[21] and are better able to probe regions closer to the elastic line. However, Raman is not suited to the detection of light species, such as vibrations arising from hydrogen–framework interactions. We note that INS is ideally suited to such investigation. Jacobs *et al.* have shown that INS is able to examine the binding of ammonium cations in exchanged zeolite Y (FAU topology),[22] and also introduced ammonia into this NH_4-Y systems. They report that some additional peaks appear at high loading, which are suggested as translational (<24 meV) and librational (24–70 meV) motions of the ammonia molecules. We have conducted this study to detect, model and definitively assign the spectra of ammonia in the presence of a coordinating cation (sodium) within a zeolite framework. We investigate low concentrations of ammonia within the zeolite, with loadings of four and eight ammonia molecules per unit cell. These concentrations are chosen to reflect the initial coordination of ammonia within the zeolite host. The spectra are shown to contain peaks relating to the vibrational modes of the coordinated ammonia, which are then assigned by density functional modeling of the system.

---

[a] *Department of Chemistry, Inorganic Chemistry Laboratory, University of Oxford, South Parks Road, Oxford, OX1 3QR, UK. E-mail: andrew.seel@chem.ox.ac.uk*
[b] *ISIS Facility, Rutherford Appleton Laboratory, Chilton, Didcot, Oxon OX11 0QX, UK*

2. Experimental section

2.1 Zeolite synthesis

All spectra collected within this study were obtained from synthetic Na-zeolite A (NaA) following a procedure from ref. 23 with slightly different starting materials. Instead of using precipitated silica, we have used Ludox SH-40 as a source of silica. 31.3 g of sodium aluminate (ABCR 99.9%), 93.3 g of deionized water, 223.45 g tetramethylammonium hydroxide solution (25% TMAOH) (Aldrich) and 90 g of Ludox SH-40 (40% silica in H_2O, Aldrich) were mixed together and stirred for 20 min. This mixture was left at room temperature for 28 h and heated at 383 K for 25 h with no agitation. After crystallisation, the resulting solution was washed with deionized water to pH $\sim$6 and dried overnight at 110 °C. The resulting product yielded about 65 g of fine white powder, which was checked by XRD. The sample was then transferred to a vacuum furnace and calcined over a period of eight hours at 673 K and a pressure of $< 10^{-4}$ mbar. The sample was stored under an inert atmosphere in an argon glovebox. Elemental analysis was performed to give an accurate composition of the sample, $Na_9Si_{15}Al_9O_{48}$.

2.2 INS technique

INS spectra were measured using the inverse geometry time-of-flight (tof) spectrometer, TOSCA, at the ISIS pulsed spallation neutron source (Rutherford Appleton Laboratory, Chilton, UK). Initially the dehydrated NaA sample was transferred to a stainless-steel can, under an inert atmosphere and sealed. A background spectrum for the dehydrated zeolite was collected at 4 K in order to minimise multiphonon effects. The temperature was then raised to 298 K, and ammonia gas was introduced into the zeolite by opening the sample to a pressure of 1 bar of ammonia *in situ*. The sample was then sealed and the temperature again lowered to 4 K for the recording of the ammoniated zeolite spectra.

The data were collected over the range 3–500 meV (24–4000 cm^{-1}) using detection banks for both forward and back scattering on TOSCA. The high intensity of neutrons at the ISIS source, coupled with long run times of 12 h for each sample minimizes the signal to noise ratio, and for all practical purposes the resolution of the instrument can be taken as 1.5% of the energy transfer (between 0.25 and 1.0 cm^{-1} over the energy range discussed). Raw spectra were converted into $S(Q, \omega)$ and manipulated using standard ISIS data treatment programs.[24] The relation between energy and momentum transfer (Q, Å^{-1}) is given by:

$$Q^2 = \frac{2m}{\hbar^2}\left(2E_f + \hbar\omega - 2\sqrt{E_f(E_f + \hbar\omega)}\cos\theta\right) \qquad (1)$$

where m is the neutron mass, θ the scattering angle, ω the angular frequency and $\hbar$ is Planck' s constant divided by 2π. Since the final energy, E_f, is fixed at 3.8 meV on TOSCA, at a given scattering angle the energy-transfer is associated with a unique momentum transfer.

2.3 Computational detail

Modelling of atomic displacements and vibrational spectra of NaA, with a specified number of ammonia molecules per unit cell, were carried out at the fully periodic density functional theory (DFT) level using the CASTEP code.[25] We took an initial framework crystal structure from the zeolite database[26] with space group symmetry $Pm\bar{3}m$ and prepared a full unit cell in $P1$ symmetry, with arbitrary distribution of Si and Al in accordance with sample stoichiometry. In order to reduce the computational demand, we pre-optimised the tetrahedral framework by geometric simulation using the GASP code.[27–29] In this method each tetrahedral unit is matched to a template with ideal tetrahedral geometry and an appropriate T–O bond length (1.61 Å for Si–O and 1.75 Å for Al–O). Atoms are tethered to the vertices of templates by harmonic constraints and the atomic coordinates and the template positions and orientations are mutually relaxed so as to minimise distortion of the constraints. This allows rapid relaxation of the polyhedral framework capturing cooperative motions of the tetrahedra. This is the first time GASP has been used as a pre-optimisation technique in density functional calculations. These relaxed frameworks were then used in the DFT calculations with ammonia molecules inserted. The unit cell dimensions were fixed in the calculations ($a = b = c = 11.9$ Å, $\alpha = \beta = \gamma = 90°$), and no symmetry constraints were implemented. The generalised gradient form of the exchange–correlation functional of Perdew, Burke and Ernzerhof (PBE) was used,[30] and a planewave cutoff of 500 eV was specified for all calculations. For a discussion of functional/plane-wave accuracy in large zeolitic systems the reader is referred to examples in the literature.[31,32] Due to the large unit cell size, calculations were confined to the Γ-point. Phonon calculations in CASTEP were performed using the finite-displacement method. All modeled spectra shown in this work were refined using the aCLIMAX code for the modelling of INS spectra.[33]

3. Results and discussion

It is found empirically that the incoherent neutron scattering cross section for hydrogen (80.26 barn) is far greater than its coherent cross section (1.7568 barn) or the cross sections of any other element in our systems.[34] In light of this, and due to the subtraction of the zeolite + can background, all spectra presented in this work are expected to be dominated by the vibrations involving the hydrogen of the absorbed ammonia.

Fig. 1 shows the INS spectra for NaA loaded with an average of four ammonia molecules per unit cell. Considering the maximum loading of ammonia in NaA detected by crystallographic techniques is thirty two,[35] a loading of four can be classified as a low concentration and be considered as indicative of initial coordination sites. As has been stated, at this concentration of ammonia the system is expected to be disordered and the distribution of ammonia inhomogeneous through the crystal. It can be seen that there are no additional peaks present in the forward-scattering spectrum, and thus all vibrational modes appearing in the spectrum are due to scattering from hydrogen. The first deduction that can be made from Fig. 1 is that the ammonia molecule is not acting

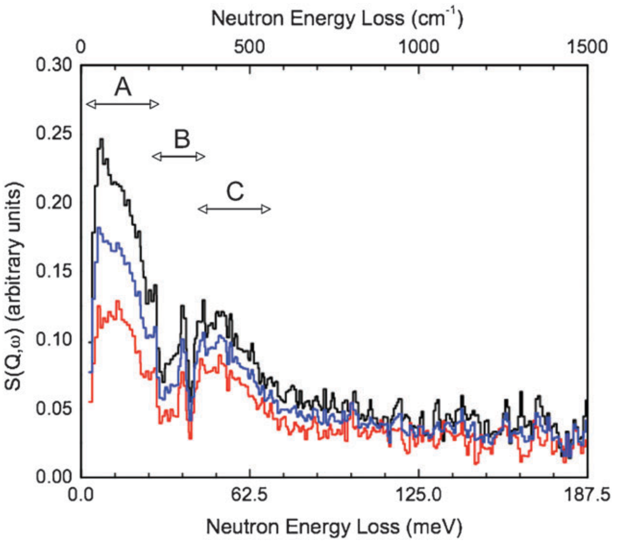

Fig. 1 INS spectra of NaA·4NH$_3$, showing forward (red), back (black) and difference average (blue) scattering. Zeolite and can backgrounds have been subtracted from the data.

as a free rotor within the zeolite cage. If that were the case, the INS spectrum would consist of very broad, gaussian peaks across an energy range of hundreds of cm^{-1} due to the effect of molecular recoil.[36] In Fig. 1 three distinct structures can be seen, which is an important result in that it indicates that INS *is* able to examine the vibrational modes of the ammonia molecule bound to the zeolite. The first structure is across the range 6–28 meV (labelled as A in Fig. 1) and seems to consist of a collection of peaks of decreasing intensity. The second region (B) consists of one peak at 38 meV, and the final structure is again a collection of peaks across a range of 43–66 meV (C). No structures were observed above 188 meV and so are not reported here.

In order to assign atomic displacements to these vibrational modes a number of calculations were carried out on model systems, as detailed in the previous section. It can be seen from Fig. 2 that there exist two pore environments in the LTA framework, one larger α-cage at the center of the unit cell, and smaller β-cages at each cell corner. Within the α-cage of a stoichiometric NaA unit cell a number, x, of ammonia molecules were distributed, and the system relaxed under periodic conditions. Calculations were performed for $x = 1$, 3 and 4. No ammonia molecules were placed within the β-cages of the zeolite, since previous studies have shown that population of these sites occurs slowly, and at very high pressures of ammonia.[38] Under our experimental conditions it is assumed no such population occurs. It should be noted that these calculations are not intended as being structurally definitive, but rather are used to assign regions in the experimental spectra.

For the $x = 4$ system, the ammonia molecules were distributed in a tetrahedral array within the α-cage, one being removed for $x = 3$ and three removed for $x = 1$. In all cases the structure relaxed with coordination of the N of ammonia to the Na$^+$ cations in the cage. It is also interesting to note that these ammonia molecules orient in such a way as to give a close approach between one H atom and a framework O-bridge. This distance of 1.8 Å is indicative of a hydrogen bond between ammonia and the framework, and is in agreement with previous NMR studies.[16,39] Fig. 3 shows the calculated INS spectra for these NaA·xNH$_3$ systems. Due to multi-quanta processes being strongly observed in INS, calculations of these overtones up to 0 → 10 were carried out, although only the total, first and second overtones are plotted.

Comparing the $x = 1$,3 and 4 spectra, it is seen that again three regions can be defined, each of which increases in range as x increases. The peak structures at lowest momentum transfer (up to 26 meV) correspond to a translational motion of the ammonia molecule perpendicular to the Na–N direction. Examining the $x = 1$ spectrum it can be seen that this occurs at 76 meV, which upon increasing x to 3 and 4 becomes a spread of peaks in the range 3–17 meV. The higher momentum transfers in this range involve the translational motion of multiple NH$_3$ molecules. The second broad peak in the calculated spectra grows from the 53 meV and 67 meV peaks in the $x = 1$ case (noting that the peaks at 41 and 50 meV are 0 → 2 overtones) and correspond to a tilting motion of the NH$_3$ molecule with an invariant Na–N distance. In the $x > 1$ spectra these two peaks become a multiple of structures between 48–62 meV. The lower end of this range corresponds to the tilt being constrained by the hydrogen bonding between ammonia and the framework, with the higher momentum transfers exciting multiple NH$_3$ molecules. Fig. 3 shows a region of sharp features which can be clearly distinguished between these two broad ranges in the calculated spectra. These are librational modes, and for the $x = 1$ case a single peak occurs at 31 meV. These three vibrational regions are shown schematically in Fig. 4, depicting the ammonia fragment as coordinated to the sodium cation, with hydrogen bonding to framework oxygen.

A comparison between calculated and experimental INS spectra is given in Fig. 5. The plot of experimental and $x = 4$ calculated spectra shows good agreement between the broad features, and the existence of a sharp peak range between them. There is, however, a noticeable lack of multiple peaks in the experimental spectrum between 25–36 meV, and there is a stark difference in intensity. The experimental peak lies at 38 meV, with some intensity appearing at slightly lower momentum transfer. With good fit between experiment and calculation for the translational and tilting regions, it remains to be explained why the librational region shows this discrepancy. The calculated spectra in this librational region show a frustrated rotation about the N–Na axis, with the lower-end momentum transfers corresponding to hindrance by the hydrogen bonding interaction between ammonia and the oxygen-bridges in the framework. This motion, more than the translational and tilting modes, is not accurately modeled by the assumptions implicit in the finite displacement techniques for the solid state employed in this work, since upon neutron impact molecular recoil appreciably affects the exponential term in eqn (2),[34,36,40] the Debye–Waller factor. Here, ν signifies a particular vibrational mode, ${}^{\nu}u$ the corresponding atomic displacement and n the order of the transition.

$$S(Q,\omega_\nu) \propto \frac{[(Q^{\nu}u)^2]^n}{n!} e^{-(Q\sum_{\nu}({}^{\nu}u))^2} \qquad (2)$$

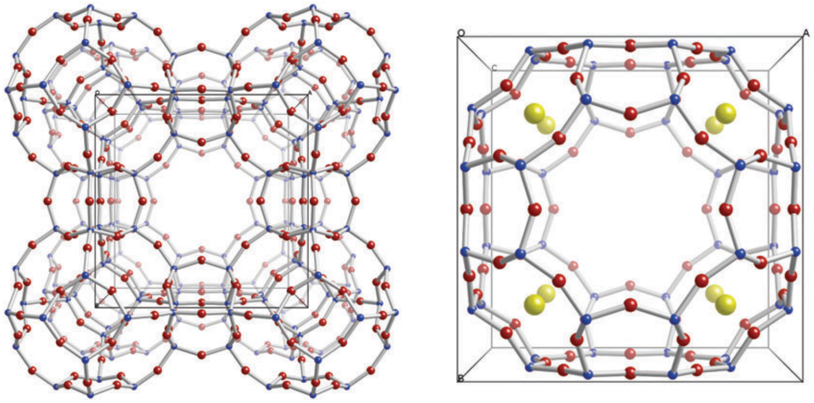

Fig. 2 Left: the pore environments of the LTA framework, displaying the central α-cage and smaller β-cages.[37] Note only the framework oxygen (red) and Si/Al (blue) are shown. Right: cation (yellow) positions in the α-cage.

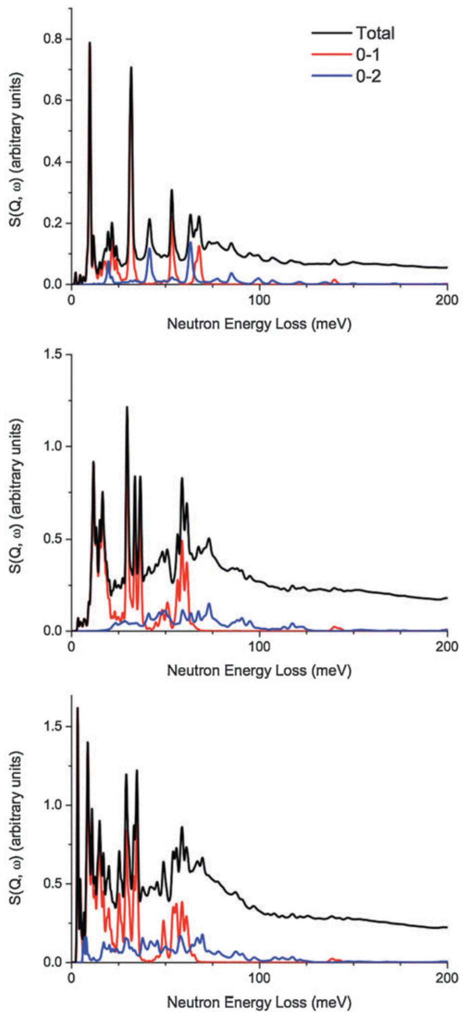

Fig. 3 Calculated INS spectra of NaA·4NH$_3$, showing total, fundamental and first overtone transitions. Top: $x = 1$, middle: $x = 3$, bottom: $x = 4$.

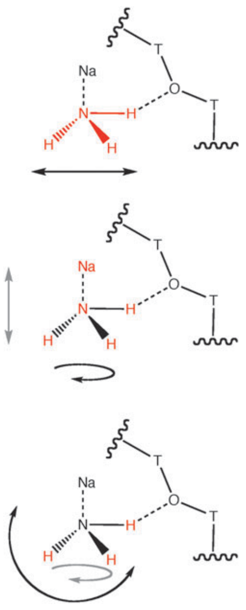

Fig. 4 Schematic of the vibrational modes of ammonia coordinated to an extra-framework sodium cation, as calculated in Fig. 3. The grey arrows represent slight displacements whilst the black arrows represent the principle displacements of the red-highlighted atoms. The label T denotes a framework silicon or aluminium centre.

For a rotor fragment the momentum transfer from incident neutron impact is treated as an interaction with a single particle of increased effective mass (compared to the rest mass of the fragment). Subsequently a greater energy neutron is needed to excite the rotor fragment, and the effect of Q is greater. This effect exhibits itself in an INS spectrum as a decrease in intensity of the vibrational mode, accompanied by a shift of intensity to wings in the higher energy momentum transfer part of the spectral line. The experimental spectra do indeed show a decrease in peak intensity, and where two delta functions appear in the calculated spectra, one peak with an intensity maximum shifted to higher wavenumber results.

Finally, Fig. 6 shows the results of the second loading of ammonia into the system, to give an average of eight ammonia molecules per α-cage. A loading of eight was chosen to examine whether ammonia coordination would occur to each cation in the α-cage before other sites were populated. Previous crystallographic studies show that for maximally loaded NaA all cation sites in the α-cage coordinate with the ammonia,[35] yet suggest that the binding of ammonia at low

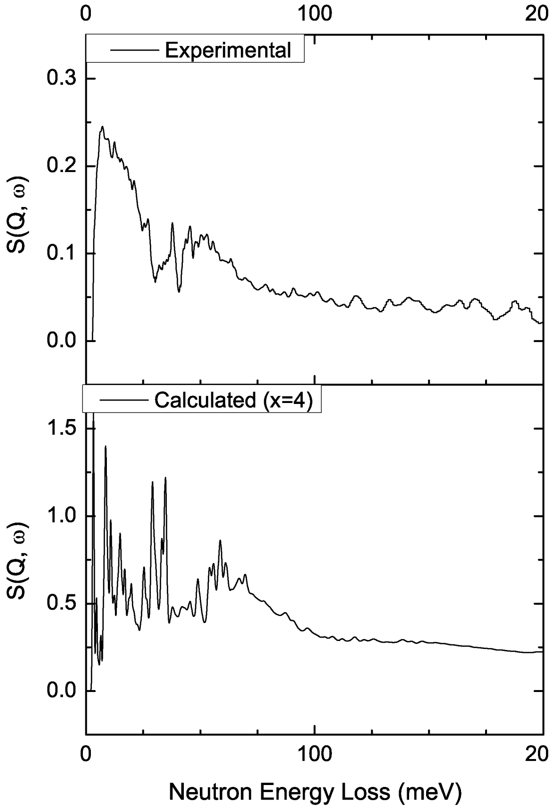

Fig. 5 Comparison between calculated and experimental INS spectra of NaA·$4NH_3$.

coverage is not specific.[41–43] It can be seen from Fig. 6 that no additional peaks appear after the second loading. The difference spectrum instead shows a low-intensity and broad feature, indicative of recoil. This would suggest that the additional ammonia molecules do not coordinate with the extra-framework cations, but rather exist as loosely bound molecules in the pore. It is unclear at this stage whether the absence of coordination to all cations in this study is due to low-loading of ammonia or experimental conditions.

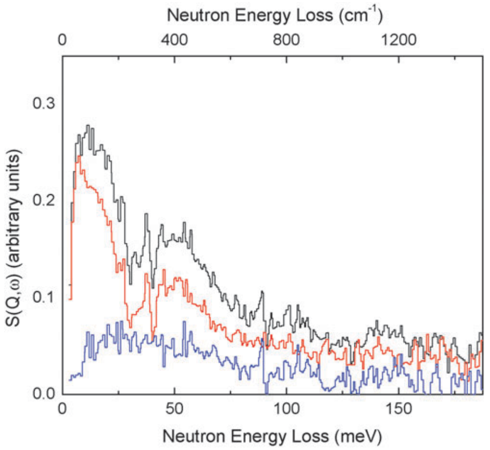

Fig. 6 INS spectra of NaA·xNH_3 showing the difference (blue) between first (x = 4, red) and second (x = 8, black) loading.

4. Conclusion

We report here the first inelastic neutron scattering data for coordinated ammonia loaded *in situ* into a microporous material. We have loaded a low concentration of ammonia (four and then eight per unit cell) into NaA zeolite, and have shown that despite the recoil effect of ammonia upon neutron impact, inelastic scattering is able to detect vibrational structure. The assignment of INS spectra has been verified by modeling techniques, combining geometric relaxation of the zeolite framework with fully periodic density functional calculation. We have assigned the INS spectra of ammonia in NaA at low coverage as consisting of a translational, librational and tilting motion, in accordance with ammonia coordination with extra-framework cations. Similarities/deviance from the calculated model have been discussed. In light of this study we have shown that INS is a valid technique to aid the study of hydrogen-containing small molecules within a zeolite framework, and suggest that further studies may now be performed for systems where alternative techniques are limited, such as NMR for paramagnetic systems.

Acknowledgements

A. Seel thanks the EPSRC and A. Sartbaeva thanks the Glasstone Research Fellowship for funding. We thank the Rutherford-Appleton Laboratory (Chiltern, Oxforshire, UK) for use of the ISIS facility, and the Oxford Supercomputer Service for the use of their Redqueen system.

References

1 A. Zecchina, S. Bordiga, J. G. Vitillo, G. Ricchiardi, C. Lamberti, G. Spoto, M. Bjorgen and K. P. Lillerud, *J. Am. Chem. Soc.*, 2005, **127**, 6361–6366.
2 R. E. Morris and P. S. Wheatley, *Angew. Chem., Int. Ed.*, 2008, **47**, 4966–4981.
3 G. Sastre and A. Corma, *J. Mol. Catal. A: Chem.*, 2009, **305**, 3–7.
4 G. A. Ozin, A. Kuperman and A. Stein, *Angew. Chem., Int. Ed. Engl.*, 1989, **28**, 359–376.
5 C. Marcilly, *J. Catal.*, 2003, **216**, 47–62.
6 A. Sartbaeva, V. L. Kuznetsov, S. A. Wells and P. P. Edwards, *Energy Environ. Sci.*, 2008, **1**, 79–85.
7 P. Moriarty and D. Honery, *Int. J. Hydrogen Energy*, 2009, **34**, 31–39.
8 P. P. Edwards, V. L. Kuznetsov and W. I. F. David, *Philos. Trans. R. Soc. London, Ser. A*, 2007, **365**, 1043–1056.
9 P. A. Anderson, *Solid State Hydrogen Storage*, 2008, 223–260.
10 A. J. Ramirez-Cuesta, P. C. H. Mitchell, D. K. Ross, P. A. Georgiev, P. A. Anderson, H. W. Langmi and D. Book, *J. Mater. Chem.*, 2007, **17**, 2533–2539.
11 R. F. Cracknell, P. Gordon and K. E. Gubbins, *J. Phys. Chem.*, 1993, **97**, 494–499.
12 U. D. Joshi, P. N. Joshi, S. S. Tamhankar, V. V. Joshi and V. P. Shiralkar, *J. Phys. Chem. B*, 2001, **105**, 10637–10647.
13 C. Zamfirescu and I. Dincer, *J. Power Sources*, 2008, **185**, 459–465.
14 A. Klerke, C. H. Christensen, J. K. Norskov and T. Vegge, *J. Mater. Chem.*, 2008, **18**, 2304–2310.
15 F. Yin, A. L. Blumenfeld, V. Gruver and J. J. Fripiat, *J. Phys. Chem. B*, 1997, **101**, 1824–1830.
16 G. P. Holland and T. M. Alam, *Phys. Chem. Chem. Phys.*, 2005, **7**, 1739–1742.
17 I. A. Beta, J. Herve, E. Geidel, H. Bohlig and B. Hunger, *Spectrochim. Acta, Part A*, 2001, **57**, 1393–1403.
18 H. Jobic, A. Renouprez, A. N. Fitch and H. J. Lauter, *J. Chem. Soc., Faraday Trans. 1*, 1987, **83**, 3199–3205.

19 C. Corsaro, V. Crupi, D. Majolino, S. F. Parker, V. Venuti and U. Wanderlingh, *J. Phys. Chem. A*, 2006, **110**, 1190–1195.
20 F. Gilles, J. L. Blin, H. Toufar, M. Briend and B. L. Su, *Colloids Surf., A*, 2004, **241**, 245–252.
21 S. Bordiga, A. Damin, F. Bonino, G. Ricchiardi, R. Tagliapietra and C. Lamberti, *Phys. Chem. Chem. Phys.*, 2003, **5**, 4390–4393.
22 W. P. J. H. Jacobs, R. A. van Santen and H. Jobic, *J. Chem. Soc., Faraday Trans.*, 1994, **90**, 1191–1196.
23 H. Robson, *Verified Synthesis of Zeolitic Materials*, Elsevier, 2nd edn, 2001, pp. 185–186.
24 D. Colognesi, M. Celli, F. Cilloco, R. J. Newport, S. F. Parker, V. Rossi-Albertini, F. Sacchetti, J. Tomkinson and M. Zoppi, *Appl. Phys. A: Mater. Sci. Process.*, 2002, **74**, s64–s66.
25 S. J. Clark, M. D. Segall, C. J. Pickard, P. J. Hasnip, M. J. Probert, K. Refson and M. C. Payne, *Z. Kristallogr.*, 2005, **220**, 567–570.
26 C. Baerlocher and L. B. McCusker, *LTA Framework*, http: //www.iza-structure.org/databases/, 2009.
27 S. A. Wells, M. T. Dove and M. G. Tucker, *J. Phys.: Condens. Matter*, 2002, **14**, 4567–4584.
28 A. Sartbaeva, S. A. Wells, M. M. J. Treacy and M. F. Thorpe, *Nat. Mater.*, 2006, **5**, 962–965.
29 G. D. Gatta, A. Sartbaeva and S. A. Wells, *Eur. J. Mineral.*, 2009, **21**, 571–580.
30 J. P. Perdew, K. Burke and M. Ernzerhof, *ACS Symp. Ser.*, 1996, **629**, 453–462.
31 G. Poulet, P. Sautet and E. Artacho, *Phys. Rev. B: Condens. Matter Mater. Phys.*, 2003, **68**, 075118.
32 R. Astala, S. M. Auerbach and P. A. Monson, *J. Phys. Chem. B*, 2004, **108**, 9208–9215.
33 A. J. Ramirez-Cuesta, *Comput. Phys. Commun.*, 2004, **157**, 226–238.
34 P. C. H. Mitchell, S. F. Parker, A. L. Ramirez-Cuesta and J. Tomkinson, *Vibrational Spectroscopy with Neutrons*, World Scientific, 2005.
35 R. Y. Yanagida and K. Seff, *J. Phys. Chem.*, 1972, **76**, 2597.
36 J. Tomkinson, *Chem. Phys.*, 1988, **127**, 445–449.
37 C. Baerlocher, W. M. Meier and D. H. Olson, *Complete Atlas of Zeolite Framework Types*, Elsevier, 2001.
38 V. Kanazirev and N. Borisova, *Zeolites*, 1982, **2**, 23–28.
39 C. A. Fyfe, D. H. Brouwer and P. Tekely, *J. Phys. Chem. A*, 2005, **109**, 6187–6192.
40 B. S. Hudson, *Vib. Spectrosc.*, 2006, **42**, 25–32.
41 R. Y. Yanagida and K. Seff, *J. Phys. Chem.*, 1973, **77**, 138–139.
42 F. Gilles, J. L. Blin and B. L. Su, *Colloids Surf., A*, 2004, **241**, 253–256.
43 F. Gilles, J. L. Blin, H. Toufar and B. L. Su, *Stud. Surf. Sci. Catal.*, 2002, **142**, 1687–1694.